IEEE Access
Multidisciplinary ⋮ Rapid Review ⋮ Open Access Journal

Received August 11, 2018, accepted October 8, 2018, date of publication October 17, 2018, date of current version November 30, 2018.

Digital Object Identifier 10.1109/ACCESS.2018.2876499

On the Evaluation of an Entropy-Based Spectrum Sensing Strategy Applied to Cognitive Radio Networks

GUILLERMO PRIETO[1], ÁNGEL G. ANDRADE[1], (Member, IEEE), DANIELA M. MARTÍNEZ[2], AND GUILLERMO GALAVIZ[1], (Member, IEEE)
[1]Facultad de Ingeniería, Universidad Autónoma de Baja California, Mexicali 21280, México
[2]Escuela de Ciencias de la Ingeniería y Tecnología, Universidad Autónoma de Baja California, Tijuana 21280, México

Corresponding author: Ángel G. Andrade (aandrade@uabc.edu.mx)

This work was supported in part by the National Council of Science and Technology (CONACyT, Mexico) through the Fondo Sectorial de Investigación para la Educación under Grant 288670.

ABSTRACT In this paper, the evaluation of a spectrum sensing strategy based on the frequency domain entropy applied to cognitive radio networks is presented. Entropy estimation is performed using Bartlett periodogram. A tradeoff between variance and the spectral resolution for Bartlett periodogram is presented. This tradeoff affects the probability of detection and false alarm of the spectrum sensing strategy in environments with low signal-to-noise ratio and noise uncertainty. The Entropy detector is optimal when the product of the number of segments and the number of points used is equal to the number of available samples of the received signal.

INDEX TERMS Cognitive radio, signal detection, entropy, Bartlett's periodogram, SNR wall.

I. INTRODUCTION

Nowadays, the widespread adoption of the idea that everyone should be communicated anywhere, anytime and using different wireless technologies has led to an exponential growth in wireless data traffic. These trends in the use of wireless data challenge the design and development of emerging applications and compromise the quality of service of current and future wireless services, since the available spectral resources may be insufficient to accommodate them all.

One approach to providing the spectral resources needed is to modify the current spectrum allocation policies to make more efficient use of the frequency bands. However, it may take several years to reuse spectrum bands for another use due to regulatory processes [1]. This motivates the development of innovative ways to exploit the radio spectrum to identify the spectral resources needed to meet future demands for wireless and mobile traffic.

By integrating capabilities such as spectrum awareness, spectrum allocation, and spectrum mobility, Cognitive Radio (CR) is considered as the potential technology to enable the so-called dynamic spectrum access by allowing smart terminals (i.e., secondary users, SUs) take advantage of unused spectrum resources of primary users (PUs) [2].

However, a real-time estimate of the presence of signals to determine if spectral resources are available becomes increasingly challenging as networks become denser and more heterogeneous. Therefore, a great effort on the design of spectrum sensing (SS) techniques that consider the heterogeneity of current and future networks is made.

To date, various SS techniques have been proposed and studied, ranging from simple energy detection (ED), cyclostationary feature detection (CFD) and the matched filter (MF) [3], to detection based on eigenvalues (EBD) [4] and covariance-based detection (CBD) [5]. Each of the proposed techniques presents a tradeoff of performance and computational complexity. Among these techniques, ED is the most implemented and studied due to its simplicity and that an acceptable performance tradeoff can be reached [6]. Furthermore, ED is able to resolve about the availability of the spectrum without prior knowledge of the primary signals, which is an attractive feature for CR applications.

However, the random and non-avoidable variation of the noise present in every wireless communication system, also known as noise uncertainty, significantly reduces the performance of ED, especially when the signal-to-noise ratio (*SNR*) is low [7]. Therefore, it is necessary to investigate other SS techniques that provide better performance with low complexity, without requiring knowledge of primary signals.

Entropy-based detection (EnBD) has recently been proposed as an interesting option for SS. It is robust to noise uncertainty and, its implementation complexity is comparable to ED since it does not require any prior knowledge of the primary signal waveform [8]–[14].

According to the information theory, entropy quantifies the predictability (or the randomness) of an event. The less predictable an event is, the higher its entropy. Therefore, the entropy of a random variable depends on its distribution. For any random variable, the maximum possible entropy occurs when it shows a uniform distribution (i.e., all its values have equal probability). Entropy, therefore, can be used as a metric for SS to determine the presence of communication signals in a channel, considering an expected statistical behavior of these signals and noise. An example of the use of entropy for SS is shown in [9], where the output of a Matched Filter is used to estimate the entropy of received signals affected by noise. Here, for a given number of sample points of the received signal, entropy reaches its maximum when the signal is composed only by noise. On the other hand, if a correlated signal is present, the entropy decreases proportionally to the *SNR* level [9].

Several works have already studied Entropy-based Detection (EnBD) for spectrum sensing in CR. Nagaraj [9] combine entropy detection in the time domain (EnBD-TD) with a matched filter. The results reported demonstrate that if a modulated signal is present the entropy of the received signal is reduced. Therefore, it allows identifying its presence. However, the detector requires perfect knowledge of the primary waveform and synchronization, so it is not suitable for CR implementations.

Zhang *et al.* [10] apply the Fourier Transform to the received signal and partition the probability space into various fixed dimensions, where the spectrum magnitude is the random variable. They demonstrate that the entropy is constant under fixed dimensions of the probability space and that the EnBD is robust to the noise uncertainty. Furthermore, the authors demonstrate that the EnBD in the frequency domain (EnBD-FD) outperforms the EnBD in the time domain (EnBD-TD). Entropy in the frequency domain is also estimated in [11], where a comparative performance analysis is carried out. The results demonstrate that the EnBD-FD provides higher sensing reliability in low *SNR* scenarios (below -15 dB) in comparison to traditional spectrum detectors (i.e., Energy and Cyclostationary Feature detectors).

The proposal in [12] analyzes the performance of EnBD-FD considering multipath fading channel. The reported results demonstrate that the performance of EnBD-FD over Rice and Rayleigh channel is comparable to that over additive white Gaussian noise (AWGN) channel. Therefore, the performance of EnDB-FD is not affected by multipath fading. Similarly, in [13] the EnBD-FD is applied for SS in cognitive radio for maritime environments. They state that the entropy detector provides the best performance for the particularly adverse characteristics of the maritime environments, as compared to other basic SS techniques.

In [14] a two-stage EnBD-FD is proposed to improve the performance of the detector reported in [11]. With this strategy, the authors reduce the computational complexity of the detector by applying the Fast Fourier Transform (FFT) algorithm to estimate the amplitude spectrum. They also conclude that if the power spectrum of the received signal is considered instead of the amplitude spectrum, the performance of the detector is improved. Nikonowicz *et al.* [15] proposed a hybrid detection. It combines the decisions made from two detectors, one based on ED and another one on EnBD-FD. However, given that the proposed scheme also relies on ED, it is still prone to the noise uncertainty effects.

According to the works analyzed above, two important remarks arise: (i) the EnBD in the frequency domain provides better performance than in the time domain and, (ii) the estimation of the spectral entropy is better when considering the power spectrum instead of the amplitude spectrum. From these remarks, it is straightforward to think that a correct estimation of the power spectrum is of paramount importance in the performance of EnBD-FD.

The periodogram is the method proposed in [14] to estimate the power spectral density (PSD). The periodogram is an asymptotically unbiased but non-consistent estimate of true PSD, as demonstrated in [16]. The lack of consistency of the estimator leads to poor quality estimate. Having in mind that the performance of the EnBD-FD depends on the accurate representation of the PSD, in this work we propose to estimate the PSD using Bartlett's periodogram [17], which is a non-parametric estimator, asymptotically unbiased and consistent. The results obtained demonstrate that if the quality of the PSD estimate is improved, the performance of the EnBD-FD is also improved.

The Bartlett periodogram is a proposed method for reducing the variance of the PSD estimate. It consists of dividing the N-point data sequence into K nonoverlapping segments, in which each segment has a length of M points. According to the analysis of the method, the reduction of the variance occurs at the expense of a reduced resolution in the PSD estimate. This is, for a given K, the variance and the spectral resolution are reduced by a factor of K, as demonstrated in [16]. This means that some of the spectral components of the true power spectrum could not be resolved in the PSD estimate.

In this work, we demonstrate that tradeoff between the variance and spectral resolution of Bartlett periodogram affects the performance of EnBD-FD. On one side, reducing the variance of PSD estimate achieves a consistent estimate of the true power spectrum, which provides a better estimate of the entropy of the received signal. On the other hand, the loss of spectral resolution would result in the loss of significant information regarding the composition of the received signal, which could turn into a poor estimation of signal's entropy. Therefore, an optimal tradeoff must be figured out according to the M and K parameters of Bartlett periodogram.

To analyze the tradeoff mentioned above, a system-level evaluation test-bed is implemented. After extensive evaluations, the obtained results allow to conclude that the best tradeoff between M and K is when $M = K$.

The rest of the article is structured as follows: In section 2, the theoretical description of EnBD-FD is presented. Section 3 briefly describes Bartlett's periodogram. The evaluation test-bed is explained in section 4, and performance results are presented in section 5. Finally, we present our conclusion and future work in section 6.

II. ENTROPY-BASED SPECTRUM SENSING

Spectrum sensing can be modeled as a binary hypothesis test problem. The hypotheses under test are:

$$H_0 : x(n) = \omega(n) \quad (1)$$

$$H_1 : x(n) = s(n) + \omega(n) \quad (2)$$

For $n = 0, 1, \ldots, N-1$. Hypotheses H_0 and H_1 stand for idle and busy frequency band, respectively.

In (1) and (2), $x(n)$, $s(n)$, and $\omega(n)$ correspond to the received signal, the modulated (primary) signal, and the noise samples, respectively, and N is the number of samples considered for spectrum sensing. $\omega(n)$ following a zero-mean Gaussian distribution with variance σ_0^2 is assumed. $s(n)$ can be a deterministic signal if a Gaussian channel is considered, or a stochastic signal with a mean μ_1 and variance σ_1^2 if a multipath fading channel is considered. It is assumed that $s(n)$ and $\omega(n)$ are independent.

Hypothesis testing is carried out by comparing a test statistic, $T(x)$, with a suitable threshold, λ, according to some rule that provides the best tradeoff among the specificity and the power of the test.

Shannon's entropy, denoted by H, is a measure of the uncertainty present in a random variable. It can be quantified by the following equation [18]:

$$H(Y) = -\sum_{i=1}^{L} p_i \, log_2(p_i) \quad (3)$$

where $\boldsymbol{Y}$ is regarded as the random variable, p_i denotes the discrete probability mass function of $\boldsymbol{Y}$, and L is the dimension of the probability space.

There exist several techniques for estimating the entropy of a random variable based on a finite number of observations. Given its reduced complexity, in this work, the histogram-based entropy estimation is considered [19].

To obtain the histogram of a data set $\mathbf{Y} = \{y_0, y_1, \ldots, y_{N-1}\}$ the range $(y_{max} - y_{min})$ of values in $\boldsymbol{Y}$ is divided into L bins with constant width A. Let n_i be the number of elements in $\boldsymbol{Y}$ falling inside the i-th bin such that, $\sum_{i=1}^{L} n_i = N$, the entropy estimate, $H(Y)$, is obtained as [14]:

$$H(Y) = -\sum_{i=1}^{L} \frac{n_i}{N} log_2 \frac{n_i}{N} \quad (4)$$

For EnBD, the detection strategy consists of testing the entropy obtained by (4) as:

$$H(Y) \underset{H_1}{\overset{H_0}{\gtrless}} \lambda \quad (5)$$

where λ is the threshold determined as in [14] by:

$$\lambda = H_L + Q^{-1}\left(1 - P_{fa}\right)\sigma_n \quad (6)$$

where

$$H_L = ln\left(2^{-1/2}L\right) + 2^{-1}\gamma + 1 \quad (7)$$

being the theoretical noise entropy, L is the number of bins, γ is the Euler-Mascheroni constant, $Q^{-1}(\cdot)$ is the inverse Q function, σ_n is the standard deviation of H under H_0, and P_{fa} is the expected probability of false alarm for the Neyman-Pearson criterion.

As discussed in [9]–[13], [15], detection techniques based on the entropy calculated from the amplitude spectrum of the received signal provides acceptable performance and are robust to the noise uncertainty. However, the performance of EnBD-FD can still be improved if the entropy is calculated from the power spectrum instead of the amplitude spectrum, as reported in [14]. Differently from [14], in this work, we propose to estimate the power density spectrum using Bartlett periodogram, because it provides a higher quality estimation of the PSD as compared to the simple periodogram.

III. BARTLETT PERIODOGRAM

In order to obtain Bartlett periodogram, the N-point data sequence $x(n)$ is divided into K nonoverlapping segments of length M. This result into the K data segments:

$$x_i(n) = x(n + iM) \quad (8)$$

for $i = 0, 1, \ldots, K-1$ and $n = 0, 1, \ldots, M-1$.

Then, the periodogram for each of the K segments is obtained as follow:

$$P_{xx}^{i}(f) = \frac{1}{M}\left|\sum_{n=0}^{M-1} x_i(n) e^{(-j2\pi fn)}\right|^2, \quad i = 0, 1, \ldots K-1 \quad (9)$$

The Bartlett periodogram is calculated by averaging the set of K periodograms obtained from (8), this is [16]:

$$P_{xx}^{B}(f) = \frac{1}{K}\sum_{i=1}^{K} P_{xx}^{i}(f) \quad (10)$$

The variance and the resolution are two parameters that define the quality of the PSD estimate. The resolution for Bartlett periodogram is defined as follows [20]:

$$Res\left\{P_{xx}^{B}(f)\right\} = \frac{0.89 * 2\pi}{M} = 0.89\frac{K * 2\pi}{N} \quad (11)$$

Meanwhile, the asymptotic variance is defined as:

$$\lim_{N\to\infty}\left[\mathrm{Var}\left\{P_{xx}^{B}(f)\right\}\right] \approx \lim_{N\to\infty}\left[\frac{1}{K}\mathrm{Var}\left\{P_{xx}^{i}(f)\right\}\right] \approx \frac{1}{K}P_{xx}^{2}(f) \quad (12)$$

From (12) it can be observed that by increasing the number of averages K in the Bartlett method, reduce the variance of the PSD estimate by the same factor. This results in a smoother representation of the true PSD. However, as K increases, the length of the data set considered for obtaining the periodograms described by (9) is reduced as N/K, resulting in a window whose spectral width has been increased by K. This, in consequence, reduces the frequency resolution by the same factor, as can be observed in (11).

Considering the tradeoff mentioned above, in this work we propose to evaluate the EnBD-FD performance according to the variance and resolution of the PSD estimate. With this, we demonstrate that the quality of the PSD estimate directly affects the performance of the EnBD-FD. The results analyzed in the following section provide insightful information on this.

IV. ANALYSIS OF THE BARTLETT'S PERIODOGRAM PARAMETERS IN ENTROPY ESTIMATION

In order to evaluate the impact of the resolution-variance tradeoff of Bartlett's periodogram in the performance of the EnBD-FD, a simulation-based testbed was designed using Numerical Simulation Software.

The structure of the testbed is depicted in the flowchart presented in Figure 1. The parameters of the simulation are summarized in Table 1. For the evaluation, several values of only noise samples (simulating the hypothesis H_0) and several values of modulated signal plus noise (simulating H_1) were generated to calculate H for each case. Each realization considers specific values for M and K in the Bartlett technique.

According to the histogram method with $L = 15$ bins, for each realization, the entropy H is estimated. In addition, the variance and the resolution of the PSD estimate are computed for each case. Tables 2 and 3 summarize the average values for H given each case of H_0 and H_1, respectively, considering different K and M values. Meanwhile, Table 4 presents the numerical difference between $H_{(H_0)}$ and $H_{(H_1)}$ for each K-M pair evaluated.

From Tables 2 and 3, we can observe that the variance of the PSD estimate decreases as K increases. This observation is valid for both cases, H_0 and H_1. It is well known, as the variance is reduced a smoothed estimate of the PSD is achieved. Similarly, the resolution decreases as K increases. Low resolution means that some of the spectral components cannot be resolved, resulting in a loss of spectral information of the received signal. These results demonstrate that there is a tradeoff between the variance and the resolution of the PSD estimate.

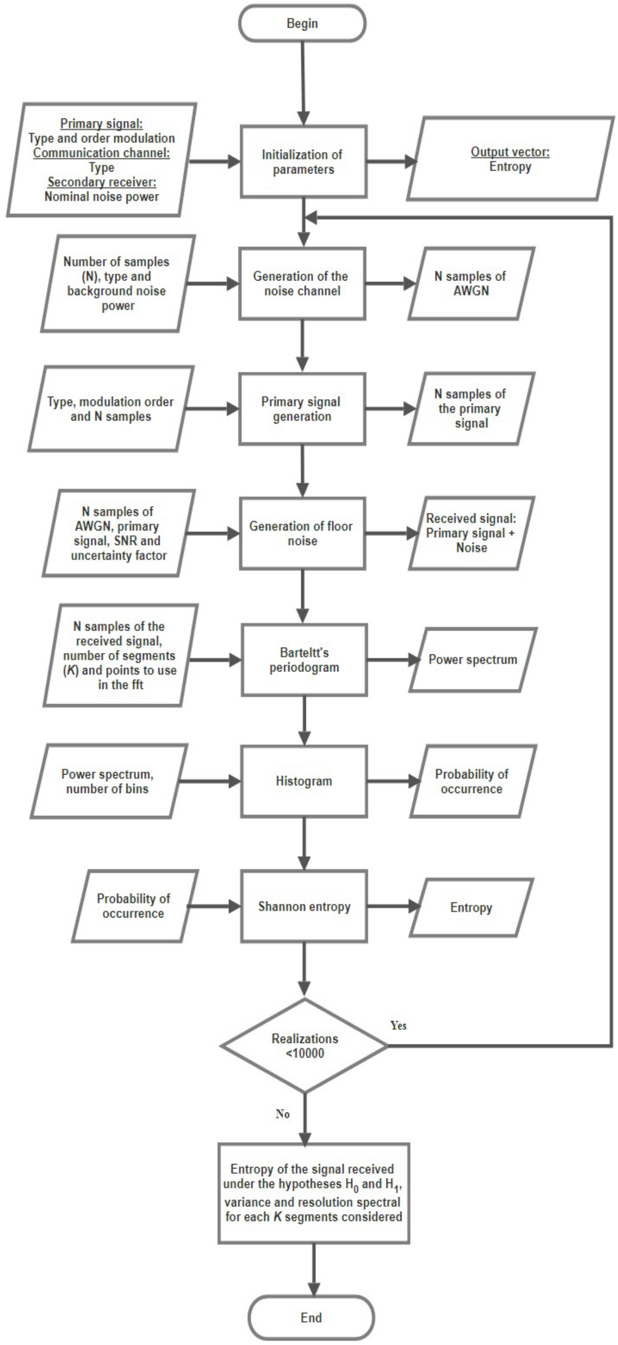

FIGURE 1. Process for estimating the variance, resolution and entropy under hypotheses H_0 and H_1.

On the other hand, to demonstrate that the tradeoff (variance and resolution) has an impact on the entropy estimate, Figure 2 presents the entropy calculated for each case of H_0 and H_1 as a function of the Resolution-to-Variance Ratio *(RVR)* for each K–M pair considered in our evaluations. The parameter *RVR* is computed as follows:

$$RVR(K, M) = log_2\left(\frac{R(K, M)}{V(K, M)}\right) \quad (13)$$

where *R(K,M)* and *V(K,M)* correspond to the resolution and variance, respectively, obtained for some K and M values.

TABLE 1. Simulation parameters.

Parameter	H_0	H_1
Signal type	AWGN	64-QAM+AWGN
Power	-90 dB	According to *SNR*
Sample Size (N)	4096	4096
Time interval (t_s)	64 µs	64 µs
Carrier frequency (f_c)	N/A	1 MHz
Sampling frequency (f_s)	N/A	$64f_c$
Data rate	N/A	1 Msymbol/sec

TABLE 2. Variance, resolution and *H values using Bartlett's periodogram under* H_0.

K	M	*Variance*	*Resolution*	$H_{(H_0)}$
1	4096	1.0618e-17	0.0014	2.3407
2	2048	5.2924e-18	0.0027	2.9003
4	1024	2.5515e-18	0.0055	3.1825
8	512	1.4008e-18	0.0109	3.3339
16	256	6.4980e-19	0.0218	3.4267
32	128	3.2359e-19	0.0437	3.4698
64	64	1.8929e-19	0.0874	3.4086
128	32	8.0271e-20	0.1748	3.1613

TABLE 3. Variance, resolution and *Hvalues, Using Bartlett's Periodogram Under* H_1.

K	M	*Variance*	*Resolution*	$H_{(H_1)}$
1	4096	1.8968	0.0014	0.2575
2	2048	1.4242	0.0027	0.3462
4	1024	1.1678	0.0055	0.4049
8	512	1.0329	0.0109	0.4274
16	256	0.9902	0.0218	0.4325
32	128	0.9658	0.0437	0.3605
64	64	0.9180	0.0874	0.2006
128	32	0.3479	0.1748	0.7846

TABLE 4. Numerical difference of entropy *H*, for H_0 and H_1.

K	M	$H_{(H_0)} - H_{(H_1)}$
1	4096	2.0832
2	2048	2.5541
4	1024	2.7776
8	512	2.9065
16	256	2.9942
32	128	3.1093
64	64	3.2080
128	32	2.3767

From figure 2 it is possible to observe that H presents an absolute maximum under H_0 and an absolute minimum under H_1. Moreover, the absolute maximum and absolute minimum are located at $K = 32$ and $M = 128$ (for H_0) and $K = 64$ and $M = 64$ (for H_1), respectively. However, from Table 4 it is observable that the largest numerical difference between $H_{(H0)}$ and $H_{(H1)}$ is when $K = M$. Therefore, it is possible to conclude that the most favorable case for differentiating among H_0 and H_1 is for $K = M$.

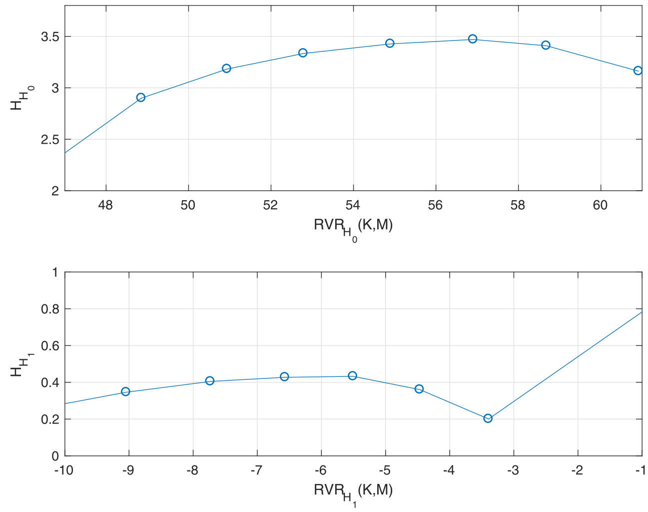

FIGURE 2. Entropy (*H*) as a function of the resolution-to-variance ratio under H_0 (top) and H_1 (bottom).

V. PERFORMANCE EVALUATION OF THE PROPOSED DETECTOR

In order to evaluate the impact of Bartlett's periodogram parameters on the EnBD performance, a system level testbed simulation was designed using numeric simulation software. The description of the testbed components is depicted in Figure 3.

The performance of EnBD-FD is evaluated by two metrics: the probability of detection P_d and the probability of false alarm P_{fa}. The P_d quantifies the ability of correctly detecting the presence of a primary signal. Meanwhile, the P_{fa} measures the possibility of erroneously detecting the presence of a primary signal when only noise is present.

The simulation parameters regarding the signals involved in the detection process have the same consideration in Table 1. Although, in this case, a factor of noise uncertainty to the noise process is added to verify that the detector is still robust to the noise uncertainty. According to the model proposed in [7], noise uncertainty is generated. The results were obtained through Monte Carlo simulations considering 10,000 realizations for each metric.

Figure 4 shows the sensibility curves for the EnBD-FD considering Bartlett periodogram. Sensitivity curves describe P_d as a function of the *SNR* of the received signal. Therefore, they allow identifying the minimum *SNR* necessary to comply with a specific P_d. The curves in Figure 4 are determined for different K and M values.

In accordance to the analysis provided in Section IV, the best performance is observed when $K = M$. This supports the initial assumption that the best performance of the EnBD-FD is achieved when the optimal tradeoff between K and M is reached.

The scheme proposed in [14] estimates H from the periodogram of the received samples. Then, H is compared to two thresholds, λ_1 and λ_2, to solve the state of the channel

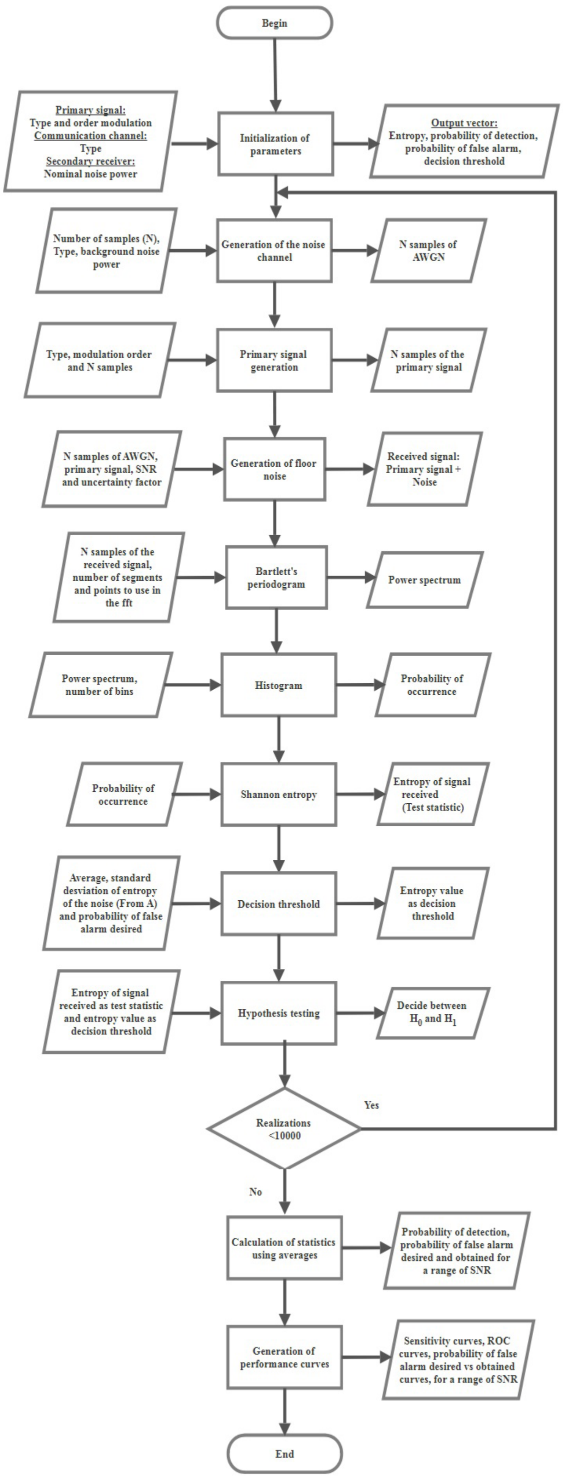

FIGURE 3. EnBD-FD with Bartlett periodogram incorporated.

of interest. The thresholds are in function of an adjustment factor Δ_0 given by $\lambda_1 = \lambda - \Delta_0$ and $\lambda_2 = \lambda + \Delta_0$, from (6) λ is calculated. If $H < \lambda_1$, the channel is busy, and if $H > \lambda_2$, the channel is considered free. However, if $\lambda_1 < H < \lambda_2$ the last two estimates of H are averaged and compared to λ, and in this way, the condition of the channel is decided.

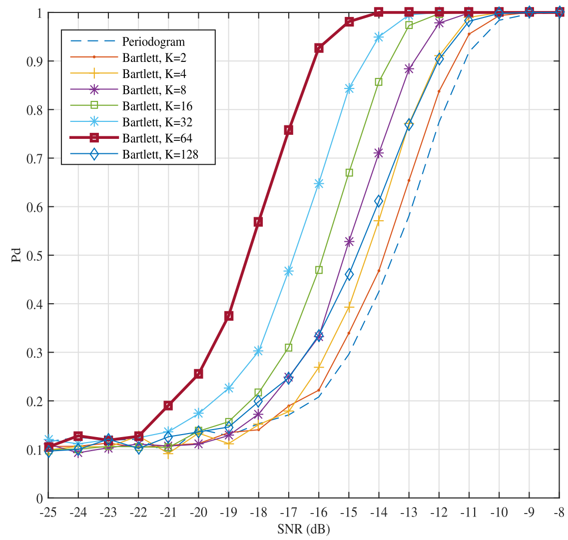

FIGURE 4. Sensitivity curves for different values of M, for a $P_{fa} = 0.1$.

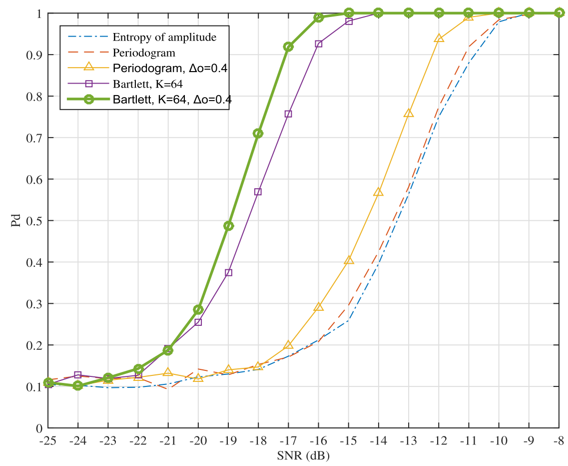

FIGURE 5. Comparison of sensitivity curves for $P_{fa} = 0.1$.

This scheme provides a better performance than that of single threshold strategies.

To validate that the scheme detection proposed in this paper is an improvement with respect to the scheme reported in [14], sensitivity curves for EnBD-FD based on the single periodogram ($EnBD - FD_P$) and EnBD-FD based on the Bartlett periodogram ($EnBD - FD_B$) are obtained (considering the simulation parameters from Table 1), the results are presented in Figure 5.

In Figure 5 it is observed that the $EnBD - FD_B$ for $K = 64$ presents a better performance as compared to the $EnBD - FD_P$. Moreover, the $EnBD - FD_B$ achieves the best performance when the double threshold strategy is applied and $\Delta_0 = 0.4$, this validates the assumptions made in Section IV. Figure 6 shows the *ROC* curves of the results shown in figure 5 for an *SNR* of -17 dB.

In order to verify the robustness of the $EnBD - FD_B$ to the noise uncertainty, the curves $P_{fa(desired)} - P_{fa(obtained)}$ are computed and presented in Figure 7. These curves describe the P_{fa} obtained by simulation as a function of the P_{fa} expected

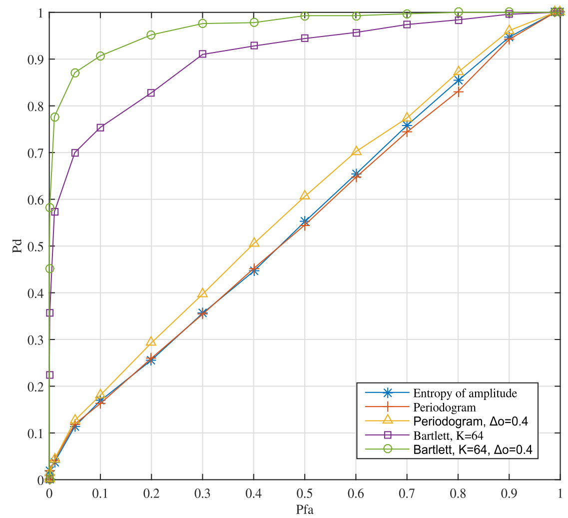

FIGURE 6. Comparison of ROC curves for *SNR* = −17 dB.

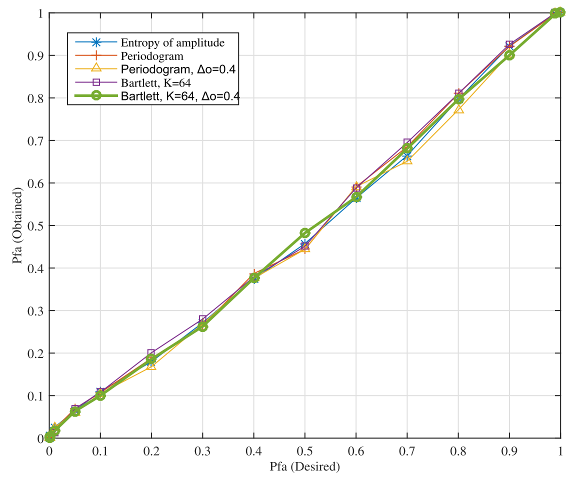

FIGURE 7. Evaluation of the P_{fa} under *UNC* = 5 dB.

or desired by the Neyman-Pearson criteria as defined in (6). For these results, we consider a noise uncertainty factor $UNC = 5$ dB.

For each EnBD-FD strategy analyzed, robustness can be observed. This is, even under the presence of uncertainty in the noise power, the P_{fa} obtained in simulations is comparable to that expected from the analytical model.

VI. CONCLUSION

In this work, the Entropy Based Detector-Frequency Domain with Bartlett's periodogram incorporated ($EnBD - FD_B$), was proposed. The tradeoff between variance and spectral resolution of Bartlett periodogram has an impact on the performance of entropy detector. It was observed that the estimation of the power spectrum of the samples of the received signal is critical depending on periodogram used, impacting the estimation of H and therefore performance $EnBD - FD_P$, when choosing between hypotheses H_0 and H_1. With Bartlett's periodogram, the variance in the estimation of the power spectrum decreases as its spectral resolution increases, it can be observed that the tradeoff between variance and resolution is optimized as K tends to $\sqrt{N}$, which considerably improves the detection performance, in terms of P_{fa} and P_d, under conditions of UNC in low SNR environments. The improvement observed in the performance of the $EnBD - FD_B$ as the variance and resolution tend to its optimal tradeoff is due to the fact that the statistical distribution of the samples received is modified, differentiating correctly between H_0 and H_1 as the SNR decreases. As a future work, we consider to evaluate the EnBD-FD applying the Welch's periodogram as a strategy to improve the estimation of the power spectrum. Welch's periodogram divides into K blocks the segment of data from the sample of the received signal; unlike the Bartlett periodogram, Welch's periodogram overlapping between blocks is allowed. In this way, the length of the sequence does not vary, as Bartlett method does, but by increasing the number of averaged periodograms, the variance is reduced. Therefore, we would expect to improve the resolution by maintaining the same variance as the Bartlett periodogram.

REFERENCES

[1] L. Zhang, M. Xiao, G. Wu, M. Alam, Y.-C. Liang, and S. Li, "A survey of advanced techniques for spectrum sharing in 5G networks," *IEEE Wireless Commun.*, vol. 24, no. 5, pp. 44–51, Oct. 2017.

[2] A. Sabbah, M. Ibnkahla, O. Issa, and Y. B. Doray, "Control channel selection techniques in cognitive radio networks: A comparative performance analysis," *J. Commun. Netw.*, vol. 20, no. 1, pp. 57–68, Feb. 2018.

[3] D. Bhargavi and C. R. Murthy, "Performance comparison of energy, matched-filter and cyclostationarity-based spectrum sensing," in *Proc. IEEE 11th Int. Workshop Signal Process. Adv. Wireless Commun. (SPAWC)*, Jun. 2010, pp. 1–5.

[4] A. Kortun, T. Ratnarajah, M. Sellathurai, C. Zhong, and C. B. Papadias, "On the performance of eigenvalue-based cooperative spectrum sensing for cognitive radio," *IEEE J. Sel. Topics Signal Process.*, vol. 5, no. 1, pp. 49–55, Feb. 2011.

[5] M. Jin, Y. Li, and H.-G. Ryu, "On the performance of covariance based spectrum sensing for cognitive radio," *IEEE Trans. Signal Process.*, vol. 60, no. 7, pp. 3670–3682, Jul. 2012.

[6] R. Umar, A. U. H. Sheikh, and M. Deriche, "Unveiling the hidden assumptions of energy detector based spectrum sensing for cognitive radios," *IEEE Commun. Surveys Tuts.*, vol. 16, no. 2, pp. 713–728, 2nd Quart., 2014.

[7] R. Tandra and A. Sahai, "Fundamental limits on detection in low SNR under noise uncertainty," in *Proc. Int. Conf. Wireless Netw., Commun. Mobile Comput.*, vol. 1, Jun. 2005, pp. 464–469.

[8] J. Nikonowicz and M. Jessa, "Blind detection methods in cognitive radio—An overview and comparison," in *Proc. 10th Int. Symp. Commun. Syst., Netw. Digital Signal Process. (CSNDSP)*, Jul. 2016, pp. 1–6.

[9] S. V. Nagaraj, "Entropy-based spectrum sensing in cognitive radio," *Signal Process.*, vol. 89, no. 2, pp. 174–180, 2009.

[10] Y. L. Zhang, Q. Y. Zhang, and T. Melodia, "A frequency-domain entropy-based detector for robust spectrum sensing in cognitive radio networks," *IEEE Commun. Lett.*, vol. 14, no. 6, pp. 533–535, Jun. 2010.

[11] Y. Zhang, Q. Zhang, and S. Wu, "Entropy-based robust spectrum sensing in cognitive radio," *IET Commun.*, vol. 4, no. 4, pp. 428–436, Mar. 2010.

[12] Y.-Y. Zhu and Y.-G. Zhu, "The simulation study of entropy-based signal detector over fading channel," in *Proc. Int. Conf. Wireless Commun. Signal Process. (WCSP)*, Oct. 2012, pp. 1–5.

[13] W. Ejaz, G. A. Shah, N. ul Hasan, and H. S. Kim, "Optimal entropy-based cooperative spectrum sensing for maritime cognitive radio networks," *Entropy*, vol. 15, no. 11, pp. 4993–5011, 2013.

[14] N. Zhao, "A novel two-stage entropy-based robust cooperative spectrum sensing scheme with two-bit decision in cognitive radio," *Wireless Personal Dec.*, vol. 69, no. 4, pp. 1551–1565, 2013.

[15] J. Nikonowicz, P. Kubczak, and L. Matuszewski, ‘‘Hybrid detection based on energy and entropy analysis as a novel approach for spectrum sensing,’’ in *Proc. IEEE Int. Conf. Signals Electron. Syst. (ICSES)*, Sep. 2016, pp. 206–211.
[16] J. G. Proakis and D. G. Manolakis, *Digital Signal Processing: Principles, Algorithms, and Applications*, 4th ed. London, U.K.: Pearson Education, 2009.
[17] M. S. Babtlett, ‘‘Smoothing periodograms from time-series with continuous spectra,’’ *Nature*, vol. 161, pp. 686–687, May 1948.
[18] C. E. Shannon, ‘‘A mathematical theory of communication,’’ *ACM SIGMOBILE Mobile Comput. Commun. Rev.*, vol. 5, no. 1, pp. 3–55, 2001.
[19] J. F. Bercher and C. Vignat, ‘‘Estimating the entropy of a signal with applications,’’ *IEEE Trans. Signal Process.*, vol. 48, no. 6, pp. 1687–1694, Jun. 2000.
[20] D. Stranneby, *Digital Signal Processing and Applications*. Great Britain, U.K.: Newnes, 2001, pp. 107–108.

GUILLERMO PRIETO received the B.S. and M. Eng. degrees in electronic engineering from the Mexicali Institute of Technology. He is currently pursuing the Ph.D. degree in electrical engineering with the Universidad Autónoma de Baja California. His research interests are in the field of cognitive radio focused on spectrum sensing.

ÁNGEL G. ANDRADE received the Ph.D. degree in electrical engineering from the CICESE Research Center, Ensenada, México, in 2005. He has over 15 years of experience in wireless and mobile communications systems. He is currently a Full Professor at the Engineering Faculty, Universidad Autónoma de Baja California, Mexicali, México. His research endeavor is focused on the sensing and opportunistic allocation of radio-frequency spectrum for cognitive radio and wireless and mobile heterogeneous networks.

DANIELA M. MARTÍNEZ received the B.S. degree in electrical engineering and the Ph.D. degree in telecommunications engineering from the Universidad Autónoma de Baja California (UABC) in 2009 and 2014, respectively. She is currently a Professor with the School of Engineering Sciences and Technology, UABC. Her research interests are within the field of statistical signal processing and cognitive radio systems.

GUILLERMO GALAVIZ received the B.S. degree in electrical engineering from the Universidad Autónoma de Baja California (UABC), the M.S. degree in electrical engineering from the University of California, San Diego, and the Ph.D. degree in electrical engineering from the CICESE Research Center, Ensenada, México. He is currently a Professor at the Mexicali Engineering School, UABC. His research interest is the scheduling of spectral resources for mobile communications systems.